Macromolecules
ARTICLE

Macromolecules **2010**, *43*, 625–629 **625**
DOI: 10.1021/ma9022313

Intermolecular Interactions and Dynamics in Polymer/C_{60} Blends

Peter A. Mirau*,† and Marjan Lyons‡

†*Nanostructural and Biological Materials Branch, Materials Manufacturing Directorate, Air Force Research Laboratory, Wright-Patterson Air Force Base, Ohio 45433 and* ‡*Wright State University, Dayton, Ohio 45431*

Received October 7, 2009; Revised Manuscript Received December 8, 2009

ABSTRACT: Solid-state NMR and X-ray scattering are used to study intermolecular interactions in miscible blends of C_{60} with polystyrene, poly(9-vinylcarbazole), and phase-separate blends with poly(ethylene oxide). Miscible C_{60} blends prepared by solution precipitation with polystyrene and poly(9-vinylcarbazole) are purple in color, show intermolecular C_{60}−polymer cross-polarization, and do not show the scattering peaks from C_{60} crystallites. The C_{60} dynamics measured using the chemical shift anisotropy filter pulse sequence shows that C_{60} rotates rapidly in the blend and averages the anisotropic line shape, while blending with C_{60} has a minor effect on the host polymer dynamics. These results demonstrate that C_{60} interacts weakly with polymers in miscible blends.

Introduction

Polymer nanocomposites have attracted great attention because materials with new and improved properties can be fabricated by combining polymers with nanometer-sized particles. The grand challenge is to combine these materials in such a way as to retain the mechanical, electrical, and optical properties of the nanoparticles while also retaining the fundamental advantages of polymers, including low cost, ease of processing, high strength, toughness, and durability.[1,2] Carbon nanotubes (CNT's) have attracted particular attention as additives because they are highly anisotropic and the tubes have unusual mechanical, electrical, and optical properties.[3] A variety of tube types (single wall, double wall, multiwall, etc.) have been identified for applications in a wide variety of polymer nanocomposite devices.

The most challenging problem in fabricating CNT composite devices is dispersing the tubes in the polymer matrix.[3,4] CNT's strongly self-associate into ropes and other higher-ordered structures that are extremely difficult to disperse in organic solvents or polymers. One possible solution is to functionalize the tubes to increase dispersibility, but this leads to changes in the CNT properties and decreased performance in nanocomposite devices. Another approach is to find solvents and/or polymers that strongly interact with the CNT's to facilitate dispersion. One goal of our research effort is identify polymers that form miscible blends with CNT's and to understand the intermolecular interactions that drive molecular level mixing.

Solid-state NMR is a powerful method to study interactions in polymer blends and nanocomposites because the chemical shifts, line widths, and relaxation times are sensitive to the structure over a local length scale (0.2−20 nm) and the dynamics over a very wide time scale (picoseconds to seconds).[5−7] To date, these methods have been used to study a variety of nanocomposites, including clay and silica nanocomposites,[8−11] but they have not been extensively used to study local interactions in CNT−polymer blends because of the difficulties in obtaining the NMR spectra of CNT's. The NMR spectra and relaxation times have been reported for CNT's,[12−14] but many preparations are difficult to study because they contain mixtures of tube types (metallic and semiconducting), mixtures of sizes, and residual paramagnetic catalysts. All of these factors tend to broaden the lines and decrease the resolution.[12,15] Furthermore, our experience shows large batch-to-batch variations in the NMR properties of CNT's.

Polymer/C_{60} blends are an ideal system to study polymer−nanoparticle interactions since C_{60} is monodisperse, available in high purity, and dispersible in many polymers[4] and block copolymers.[16,17] While there are some applications, including photovoltaics,[18] where the structure and dynamics of polymer/C_{60} blends are of direct interest, we have used C_{60} as a model system to understand the interactions between polymers and CNT's. The observation that antifullerene IgG monoclonal antibodies recognize single wall carbon nanotubes[19,20] demonstrates that C_{60} shares many structural features with CNT's and can be used to understand how macromolecules interact with CNT's.

The physical properties of polymer−C_{60} blends, including polystyrene,[4,21−23] poly(methyl methacrylate),[24] poly(dimethylphenylene oxide),[25] and tetramethylpolycarbonate,[21] have been the subject of several studies. A review of the reported results reveals that the properties depend critically on the method of blend preparation. It has been reported, for example, that low concentrations of C_{60} in polystyrene can either increase[21,26] or decrease[22,27] in the glass transition temperature (T_g) of the host polymer. It has also been reported that the best blend dispersion is observed when the components are rapidly precipitated from solution.[4]

In these studies we use rapid precipitation to prepare blends of C_{60} with polystyrene, poly(9-vinylcarbazole), and poly(ethylene oxide). Solid-state NMR and X-ray scattering are used to measure the degree of mixing, to examine the interaction strength between C_{60} and polymers, and to evaluate the effect of blending on the C_{60} and polymer dynamics. To examine the C_{60} dynamics in the blend, we have used a novel application of the chemical shift anisotropy (CSA) filter[28] to measure the degree to which the anisotropic carbon line shapes are averaged by molecular motion in the blend. The more traditional NMR measures of polymer dynamics, including the carbon spin−lattice relaxation times and dipolar line shapes, are used to evaluate how the presence of C_{60} alters the polymer dynamics on the microsecond and millisecond time scale.

*Corresponding author. E-mail: peter.mirau@wpafb.af.mil.

Published on Web 12/31/2009

Materials and Methods

Materials. Polystyrene (M_w = 288 000 g/mol), poly(ethylene oxide) (M_w = 900 000 g/mol), poly(9-vinylcarbazole) (M_w = 25 000−50 000 g/mol), C_{60}, methanol, and benzene were obtained from Aldrich and used without further purification.

Blend Preparation. C_{60}−polymer blends were prepared by solution precipitation from benzene into cold methanol. In a typical experiment 0.02 g of C_{60} was mixed with 0.2 g of polymer in 20 mL of benzene with stirring. The deep purple polymer/C_{60} solutions were precipitated with cold methanol, filtered, and dried in a vacuum oven at 60 °C. The mol % C_{60} in the blends with polystyrene, poly(9-vinylcarbazole), and poly(ethylene oxide) were 1.4, 2.7, and 0.6 mol %, respectively. Precipitation appears to be quantitative so we estimate that the C_{60} concentration is accurate to 0.1 mol %.

X-ray Diffraction. The X-ray diffraction spectra of the polymers and C_{60} blends were measured on a Bruker AXS D8 Discover and a Molecular Metrology SAXS in transmission mode.

Solid-State NMR. Solid-state NMR spectra were acquired on a Bruker Avance NMR spectrometer at 400.13 MHz for protons and 100.62 MHz for carbons, using a 7 mm magic-angle spinning probe with a spinning speed of 5−6 kHz. The 90° pulse widths were 5 μs for carbons and protons, and the signals were recorded with two-phase pulse modulation (TPPM) decoupling.[29] In some experiments the spinning side bands were suppressed using the TOSS pulse sequence.[30] The pulse sequences for the relaxation time measurements,[6] wide line correlation NMR,[31] and the CSA filter are reported in the literature.[28]

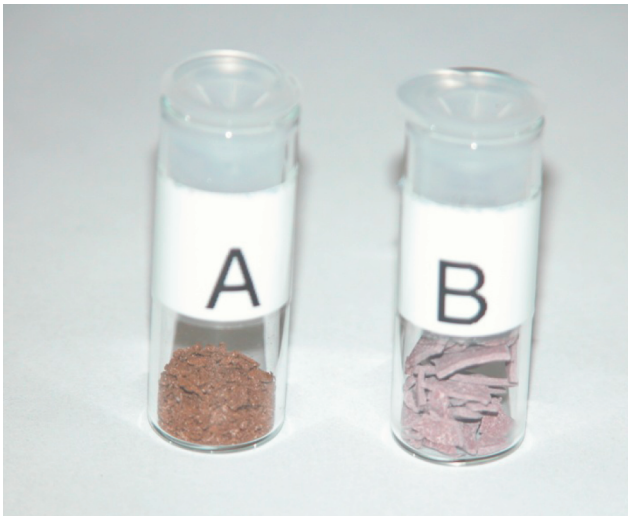

Figure 1. Photograph showing solution-precipitated blends of (A) 0.6 mol % poly(ethylene oxide)/C_{60} and (B) 1.4 mol % polystyrene/C_{60}.

Results

Solution-precipitated polymer/C_{60} blends are used as a model system to understand how CNT's interact with polymers. The dispersion can be evaluated by X-ray scattering and the precipitate color, since semicrystalline or aggregated C_{60} is a brownish color, while dispersed C_{60} is purple. The C_{60} solution mixtures with polystyrene, poly(9-vinylcarbazole), and poly(ethylene oxide) in benzene are all an intense purple color in solution, but different colored solids are observed after solution precipitation with methanol. The precipitated polystyrene and poly(9-vinylcarbazole) blends are light purple, while poly(ethylene oxide) blends give rise to a brown precipitate, as shown in Figure 1.

C_{60} dispersion in the polymer blends has been investigated by X-ray scattering, and Figure 2 compares the scattering profile for semicrystalline C_{60}, polystyrene, and the 1.4 mol % C_{60}/polystyrene blend. Crystalline C_{60} gives rise to a peak at $2\theta = 11°$ corresponding to the C_{60} diameter (0.8 nm). No scattering peaks are observed in this range for polystyrene or the purple precipitate from the C_{60}/polystyrene blend, while the crystalline C_{60} peak at $2\theta = 11°$ is observed for the brown poly(ethylene oxide) blend (not shown). These data support our conclusion that the purple solids contain dispersed C_{60} while the brown solids contain aggregated C_{60}.

Cross-polarization NMR has been effectively used to study intermolecular association in polymers and other materials.[6,7,32] The cross-polarization pulse sequence begins with proton magnetization that is transferred to carbons during a spin-lock (or cross-polarization) period. This method is ideally suited to investigate C_{60} blends because C_{60} does not contain protons and cannot be cross-polarized unless it is in close proximity to the polymer protons.[33]

Figure 3 shows the solid-state carbon spectra for the 1.4 mol % solution-precipitated blend of C_{60} and polystyrene. At short cross-polarization times, only the polystyrene signals, including the nonprotonated carbons at 146 ppm, the protonated aromatic carbons at 128 ppm, and the overlapping methine/methylene

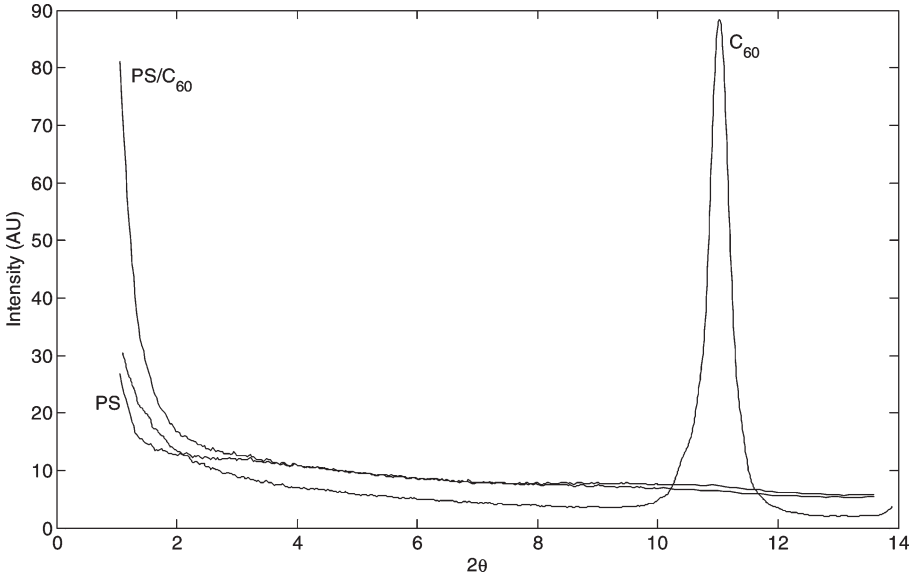

Figure 2. X-ray scattering for bulk C_{60}, solution-precipitated polystyrene, and solution-precipitated 1.4 mol % polystyrene/C_{60}.

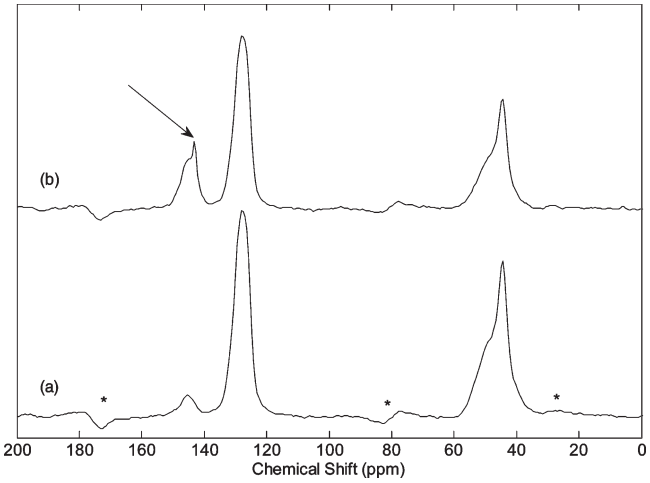

Figure 3. The 100 MHz carbon solid-state NMR spectra of the solution-precipitated polystyrene/C_{60} acquired with cross-polarization contact times of (a) 0.1 and (b) 5 ms. The peak at 143 ppm in spectrum b is assigned to C_{60}. The spinning sidebands (*) were partially suppressed with the TOSS pulse sequence,[30] and the arrow shows the peak position of C_{60}.

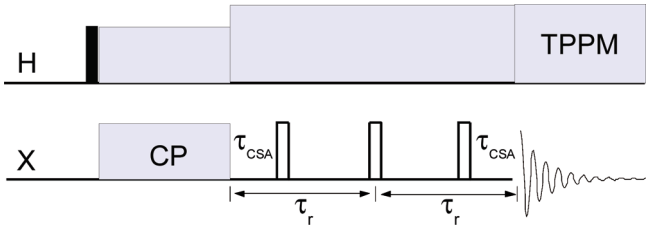

Figure 4. Pulse sequence diagram for the chemical shift anisotropy filter.[28]

carbon peak at ~40 ppm, are observed. At cross-polarization times longer than 2 ms a sharp peak at appears 143 ppm, the chemical shift reported for C_{60} in solution.[34] It is well-known from previous studies of polymers that peaks appearing at long cross-polarization times have weaker dipolar interactions, either from longer carbon−proton distances or from partial averaging of the dipolar couplings by molecular motion.[7]

The dynamics of C_{60} in miscible blends with polystyrene and poly(9-vinylcarbazole) were investigated with the chemical shift anisotropy (CSA) filter pulse sequence shown in Figure 4.[28] The CSA filter is a recoupling experiment in which π pulses applied at specific points during the magic-angle spinning rotor cycle (τ_r) lead to dephasing and signal losses that depend on the width of the CSA line shape. The signal intensity (and phase) of the filtered signal depends on the time allotted for CSA dephasing (τ_{CSA}) and the width of the pattern. With a dephasing time of 70 μs (τ_{CSA} = 35 μs) signals from carbons with broad CSA line shapes will be greatly attenuated and negative in phase, while carbons with smaller anisotropies will appear slightly attenuated and positive in phase.[28] The CSA filter can be used to distinguish between mobile and immobile phases in those cases where the molecular motion averages the CSA line shape.

The dynamics of crystalline C_{60} have been previously investigated by solid-state carbon NMR.[35] At low temperature (T < 140 K) a broad CSA line shape is observed for C_{60} that has a width of 180 ppm (~18 kHz at a magnetic field of 9.4 T). At higher temperature a narrow, motionally averaged peak is observed that increases in intensity with increasing temperature and becomes the dominant spectral feature above 160 K. The narrow line is assigned to C_{60} in the crystalline lattice that is undergoing rapid isotropic reorientation. When the rate of molecular motion is much greater that the width of the CSA line

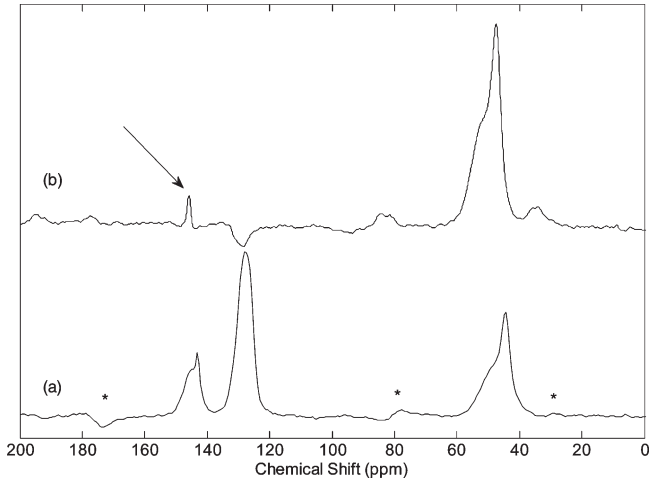

Figure 5. Solid-state carbon spectra of the polystyrene/C_{60} blend (a) without and (b) with the CSA filter. The arrow shows the peak position of C_{60} and the spinning sidebands are marked with an asterisk (*).

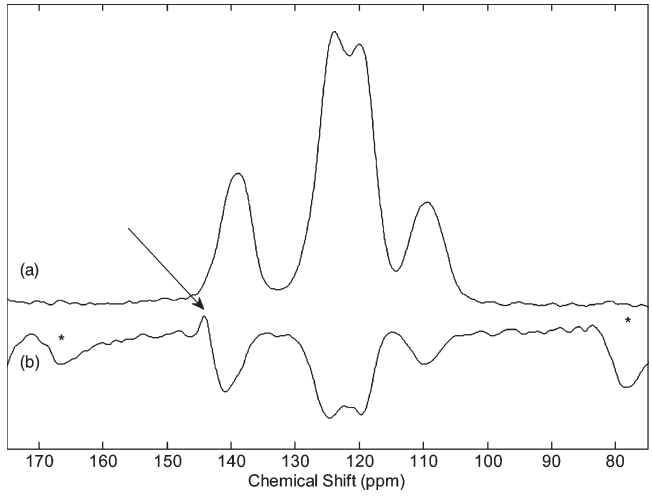

Figure 6. Solid-state carbon NMR spectra of the 2.7 mol % poly(9-vinylcarbazole)/C_{60} blend (a) without and (b) with the CSA filter. The arrow shows the peak position for C_{60} and spinning sidebands are marked with an asterisk (*).

shape (18 kHz), a single narrow Lorentzian line (LW ~ 200 Hz) is observed.

Molecular motion of C_{60} in the polymer blends can be measured from the CSA filter experiments if molecular motion averages the CSA line shape. C_{60} has a broad CSA line width in the immobile state and exhibits behavior similar to the protonated and nonprotonated aromatic carbon signals from polystyrene in the CSA filter experiment. Figure 5 compares the carbon cross-polarization spectra for the 1.4 mol % polystyrene/C_{60} blend with the CSA-filtered spectrum. As expected, the peaks with broad CSA line shapes from the polystyrene aromatic signals are greatly suppressed and slightly negative in the CSA filtered spectrum.[28] The signals from the methine/methylene peaks in the main chain have a smaller CSA line width and appear as large positive signals. The most important feature to note is the appearance of a positive signal at 143 ppm from the C_{60}. Positive signals only appear if the CSA has been effectively averaged by rapid molecular motion in the blend. These data show that C_{60} is very mobile in the miscible blend and imply that it is weakly interacting with the polymer.

Figure 6 compares the aromatic region of the solid-state carbon NMR spectrum for the poly(9-vinylcarbazole)/C_{60} blend

Table 1. Carbon Relaxation Times and Dipolar Line Widths from Polystyrene and the 1.4 mol % C_{60}/Polystyrene Blend

	polystyrene		polystyrene/C_{60}	
parameter	δ_C = 128	δ_C = 40	δ_C = 128	δ_C = 40
T_1 (s)[a]	17.1	30.2	17.2	28.5
$\Delta\upsilon_{1/2}$ (kHz)[b]	34.4	43.7	28.3	34.9

[a] The estimated uncertainty in the T_1 's is ±10%. [b] The estimated uncertainty in the diplar line widths is 3 kHz.

with the CSA filtered spectrum. The results are more difficult to interpret because the C_{60} peak overlaps with a large number of nonprotonated carbazole signals, but a weak positive signal can still be observed at 143 ppm. As with the polystyrene blend, the positive signal shows that the C_{60} is rotating rapidly in the miscible polymer blend and therefore interacting weakly.

The CSA filter experiments are sensitive to the C_{60} dynamics but do not provide information about the effect of C_{60} on the polymer molecular dynamics. To evaluate the polymer dynamics, we have measured the carbon spin−lattice relaxation times (T_1's)[7,36] and the proton dipolar line widths using two-dimensional wide-line correlation spectroscopy[31] with Lee−Goldberg cross-polarization[37] to suppress spin diffusion during the line width measurements.[38,39]

The carbon T_1's and proton dipolar line widths are sensitive to molecular motions over different frequency ranges. The T_1's are sensitive to molecular motions with a correlation time near the carbon Larmour frequency (125 MHz) while the proton line widths are can be averaged by motions faster than the dipolar line width (~50 kHz). The results listed in Table 1 show that the carbon relaxation times are insensitive to the presence of C_{60} while the proton line widths are reduced by 17−20% in the presence of C_{60}. These data are consistent with suggestions that the dynamics of polystyrene on the microsecond−millisecond time scale are sensitive to the presence of C_{60}.[21,23]

Discussion

NMR is a powerful method to study intermolecular interactions because the NMR parameters are sensitive to local (< 2 nm) structure, and a variety of relaxation and line shape experiments can be used to measure the dynamics over a wide frequency range.[6,7] To the extent that separate signals can be resolved for the polymer and nanoparticle, NMR can be used to probe the properties of both components. NMR experiments have been effectively used to characterize nanoparticle dispersion in composites and to probe the structure and dynamics of the interface.[8,9,36,40] In the case of C_{60} blends with aromatic polymers there is generally overlap between the nonprotonanted carbons and the C_{60} peak. We have overcome this limitation by using the CSA filter experiment to observe the C_{60} signals selectively. Since the C_{60} is present only at 0.6−2.7 mol %, the cross-polarization spectrum is dominated by the polymer signals, and we can use the traditional NMR methods to probe the polymer dynamics. Cross-polarization has also been used to demonstrate that C_{60} is localized to the polystyrene phase in polystyrene-*b*-poly(dimethylsiloxane) copolymer blends.[17]

The CSA filter is a recoupling pulse sequence[28] that allows us to distinguish peaks based on the anisotropic line widths. It is well-known that aromatic and carbonyl carbons have large anisotropies in the carbon spectrum and that molecular motion above T_g leads to averaging of the CSA line shapes.[6,7] Here we use the averaging of the CSA line shapes to monitor the dynamics and infer something about the strength of the polymer−C_{60} interaction. The results from the CSA filter experiment shows positive peaks for C_{60} in the miscible blends with polystyrene and negative peaks for the protonated and nonprotonated ring carbons. This demonstrates that rapid molecular motion averages the C_{60} CSA line shape but that the presence of C_{60} does not lead to a sufficiently rapid reorientation of the polystyrene aromatic ring to average the polymer CSA line shapes. The presence of C_{60} at 1.4−2.7 mol % does not change the carbon spin−lattice relaxation times but narrows the dipolar line widths. The decrease in the dipolar line width is attributed to increased molecular motion in the blend.

The effect of C_{60} on the physical properties of blends has been the subject of a number of experimental studies. Most of these literature reports are for fullerene derivatives, including PCBM, that are of interest for bulk heterojunction organic photovoltaic devices.[18] The properties of the C_{60} blends are expected to depend strongly on the length scale of mixing, so different results may be expected for the phase-separated films prepared by solvent evaporation and the miscible blends prepared by rapid precipitation.[4] As in the T_g studies mentioned previously, the dynamics probed by incoherent neutron scattering also appear to depend on blend preparation. Blends prepared by solvent evaporation show slower dynamics relative to polystyrene when detected by neutron scattering,[21] while miscible blends prepared by rapid precipitation show an increase in molecular motion.[23] As with the neutron scattering results on the miscible blends, the NMR line shape experiments are consistent with an increase in polymer molecular motion in the presence of C_{60}. This could be attributed either to a direct interaction with the C_{60} or a change in the packing efficiency in the blend.

Acknowledgment. We thank Gary Price for assistance with the X-ray and Drs. Richard Vaia and Hilmar Koerner for helpful discussions.

References and Notes

(1) Krishnamoorti, R.; Vaia, R. A. *J. Polym. Sci., Part B: Polym. Phys.* **2007**, *45* (24), 3252–3256.
(2) Vaia, R. A.; Maguire, J. F. *Chem. Mater.* **2007**, *19*, 2936–2751.
(3) Smalley, R. E.; Dresselhaus, M. S.; Dresselhaus, G.; Avouris, P. *Carbon Nanotubes: Synthesis, Structure, Properties and Applications*; Springer: New York, 2001.
(4) Mackay, M. E.; Tuteja, A.; Duxbury, P. M.; Hawker, C. J.; Van Horn, B.; Guan, Z.; Chen, G.; Krishnan, R. *Science* **2006**, *311*, 1740–1743.
(5) Abragam, A. *Principles of Nuclear Magnetism*; Oxford University Press: New York, 1961.
(6) Mirau, P. *A Practical Guide to the NMR of Polymers*; John Wiley & Sons: Hoboken, 2004; p 418.
(7) Schmidt-Rohr, K.; Speiss, H. W. *Multidimensional Solid-State NMR and Polymers*; Academic Press: New York, 1994; p 478.
(8) Hou, S.-S.; Bonagamba, T. J.; Beyer, F. L.; Madison, P. H.; Schmidt-Rohr, K. *Macromolecules* **2003**, *36*, 2769.
(9) Metin, B.; Blum, F. D. *J. Chem. Phys.* **2006**, *125* (5), 054707.
(10) Urbanczyk, L.; Hrobarikova, J.; Calberg, C.; Jerome, R.; Grandjean, J. *Langmuir* **2006**, *22* (10), 4818–4824.
(11) VanderHart, D. L.; Asano, A.; Gilman, J. W. *Macromolecules* **2001**, *34*, 3819.
(12) Goze-Bac, C.; Latil, S.; Lauginie, P.; Jourdain, V.; Conard, J.; Dulaux, L.; Rubio, A.; Bernier, P. *Carbon* **2002**, *40*, 1825–1842.
(13) Hayashi, S.; Hoshi, F.; Ishikura, T.; Yumura, M.; Oshima, S. *Carbon* **2003**, *41*, 3047–3056.
(14) Tang, X. P.; Kleinhammes, A.; Shimoda, H.; Fleming, L.; Bennoune, K. Y.; Sinha, S.; Bower, C.; Zhou, O.; Wu, Y. *Science* **2000**, *288*, 492–494.
(15) Marques, M. A. L.; d'Avezac, M.; Mauri, F. *Phys. Rev. B* **2006**, *73*, 125433−125433-6.
(16) Laiho, A.; Ras, R. H. A.; Valkama, S.; Ruokolainen, J.; Osterbacka, R.; Ikkala, O. *Macromolecules* **2006**, *39*, 7648–7653.
(17) Waller, J. H.; Bucknall, D. G.; Register, R. A.; Beckham, H. W.; Leisen, J.; Campbell, K. *Polymer* **2009**, *50*, 4199–4204.
(18) Sariciftci, N. S.; Smilowitz, L.; Heeger, A. J.; Wudl, F. *Science* **1992**, *258*, 1474–1476.
(19) Braden, B. C.; Goldbaum, F. A.; Chen, B.-X.; Kirschner, A. N.; Wilson, S. R.; Erlanger, B. F. *Proc. Natl. Acad. Sci. U.S.A.* **2000**, *97*, 12193–12197.

(20) Erlanger, B. F.; Chen, B.-X.; Zhu, M.; Brus, L. *Nano Lett*. **2001**, *1* (9), 465–467.
(21) Kropka, J. M.; Garcia Sakai, V.; Green, P. F. *Nano Lett*. **2008**, *8* (4), 1061–1065.
(22) Polotskaya, G. A.; Gladchenko, S. V.; Zgonnik, V. N. *J. Appl. Polym. Sci*. **2002**, *85* (14), 2946–2951.
(23) Sanz, A.; Ruppel, M.; Douglas, J. F.; Cabral, J. T. *J. Phys.: Condens. Matter* **2008**, *20*, 104209.
(24) Kropka, J. M.; Putz, K. W.; Pyramitsyn, V.; Ganesan, V.; Green, P. F. *Macromolecules* **2007**, *40*, 5424–5432.
(25) Biryulin, Y. F.; Melenevskaya, E. Y.; Mikov, S. N.; Orlov, S. E.; Petrikov, V. D.; Syckmanov, D. A.; Zgonnik, V. N. *Semiconductors* **2003**, *37* (1), 108–111.
(26) Weng, D.; Lee, H. K.; Levon, K.; Mao, J. D.; Scrivens, W. A.; Stephens, E. B.; Tour, J. M. *Eur. Polym. J*. **1999**, *35*, 867–878.
(27) Bershtein, V. A.; Egorov, V. M.; Zgnnok, V. N.; Melenevskaya, E. Y.; Vinogradova, L. V. *J. Therm. Anal. Calorim*. **2000**, *59*, 23.
(28) Mao, J. D.; Schmidt-Rohr, K. *Solid State Nucl. Magn. Reson*. **2004**, *26*, 36–45.
(29) Bennett, A. E.; Rienstra, C. M.; Auger, M.; Lakshimi, K. V.; Griffin, R. G. *J. Chem. Phys*. **1995**, *103*, 6951–6958.
(30) Dixon, W. T. *J. Chem. Phys*. **1982**, *77*, 1800–1809.
(31) Schmidt-Rohr, K.; Clauss, J.; Spiess, H. *Macromolecules* **1992**, *25*, 3273–3277.
(32) Schaefer, J.; Sefcik, M. D.; Stejskal, E. O.; McKay, R. A. *Macromolecules* **1981**, *14*, 188–192.
(33) Li, M.; Chen, Q. *Polymer* **2003**, *44* (9), 2793–2798.
(34) Johnson, R. D.; Meijer, G.; Bethune, D. S. *J. Am. Chem. Soc*. **1990**, *112*, 8983–8984.
(35) Tycko, R.; Dabbagh, G.; Fleming, R. M.; Haddon, R. C.; Makhija, A. V.; Zahurak, S. M. *Phys. Rev. Lett*. **1991**, *67*, 1886–1889.
(36) Mirau, P. A.; Serres, J. L.; Jacobs, D.; Garrett, P. H.; Vaia, R. A. *J. Phys. Chem. B* **2008**, *112*, 10544–10551.
(37) Lee, M.; Goldberg, W. I. *Phys. Rev. A* **1965**, *140*, 1261.
(38) Oliver, S. L.; Titman, J. J. *J. Magn. Reson*. **1999**, *140*, 235–241.
(39) Qiu, X.; Mirau, P. A. *J. Magn. Reson*. **2000**, *142* (1), 183–189.
(40) Wang, L. Q.; Liu, J.; Bordia, R. *J. Phys. Chem. B* **2000**, *104* (13), 2810–2816.